

SUPPORTING INFORMATION FOR

Interfacial Self-assembly of Gold Nanoparticle-Polymer Nanoconjugates into Microcapsules with Near-Infrared Light Modulated Biphasic Catalysis Efficiency

Jiaojiao Su^a, Shengliang Wang^a, Zhijun Xu^a, Guangyu Wu^b, Lei Wang^a and Xin Huang^{*a}

^a. MIIT Key Laboratory of Critical Materials Technology for New Energy Conversion and Storage, School of Chemistry and Chemical Engineering, Harbin Institute of Technology, Harbin, 150001, P. R. China.

^b. College of Biology and the Environment, Nanjing Forestry University, Nanjing, 210037, P.R. China

E-mail: xinhuang@hit.edu.cn.

1. Materials

HAuCl₄ · 3H₂O (99%), trisodium citrate (99%) and tannic acid (99%) were purchased from Aladdin. 2-(Dodecylthiocaroonothioylthio)-2-methylpropionic acid N-hydroxy-succinimide ester (RAFT, 98%), 2-ethyl-1-hexanol (EH, Sigma, ≥98%), 2,2'-Azobis(2-methylpropionitrile) (AIBN, Sigma, 98%), N, N-dimethyl-Formamide (DMF, Aladdin, 99%), mPEG2k-SH (98%) were purchased from Sigma-Aldrich. N-isopropylacrylamide (NIPAAm, Sigma, 98%) was recrystallized twice in hexane and toluene prior to use. Alkaline phosphatase orthophosphoric-monoester phosphohydrolase (ALP, Sigma, 10 DEA units mg⁻¹), 4-Nitrophenol (4-NP, Aladdin, 98%), 4-Nitrophenyl phosphate disodium salt hexahydrate (pNPP, Aladdin, 98%), Trolamine (TEA, Aladdin, 99%), magnesiumchloridehexahydrate (MgCl₂, Aladdin, 99%), p-Nitrophenyl butyrate (pNPB, Aladdin, 98%), dimethyl sulfoxide (DMSO, Aladdin,99%), fluorescein isothiocyanate isomer I (FITC, Sigma, 90%), all chemical reagents were used as received without further purification. Milli-Q water was used in all experiments. All glassware was cleaned and stored at drying oven before use.

2. Characterization methods

Low-magnification transmission electron microscopy (TEM) images were performed on a JEOL 2010 at 120 kV. High-resolution TEM images were acquired on a Tecnai G2 F30 operated at 200 kV. The Samples for TEM measurement were prepared by adding several drops of the dispersion on copper grid. Scanning electron microscope image were captured by using a FE-SEM SU8000 instrument (Hitachi Co.). Samples were prepared by adding a sample dilution to the wafer and vacuum drying. The sample was subjected to gold spray treatment (thickness of about 10-15 nm). Atomic force microscopy is an assembled system¹. Atomic force microscopy (AFM) images were obtained by dropping gold nanoparticle microcapsules solution onto a clean silicon wafer. The half opening angle of the tip is 45°. The spring constant of the cantilever is determined using the method proposed by Sader et al². The value is 0.006 N/m. The relationship between force and deformation of the AFM probe is in accordance with Hooke's law. That is to say, when a small force is applied to the cantilever, a suitable deformation can be detected. At the same time, the probe stiffness needs to be close to the stiffness of the sample. When the deformation of the probe caused by force is almost the same as the deformation of the sample itself, the surface morphology and mechanical properties of the sample are most similar to the actual situation. Microcapsules deformation conforms to the improved Hertz model because of low loading rate and microcapsules deformation less than half the height of the microcapsules. The apparent Young's modulus E of the microcapsules is related to the position of the contact point between the microcapsules surface, the tip and the slope of the force-distance curve. The improved Hertz model of rigid cone and plane can be expressed as

$$F = \frac{\pi}{2} \frac{E t \alpha}{(1 - \nu^2)} \cdot \delta^2$$

Where F represents the force of the probe, ν represents the unit with a Poisson's ratio of 0.5 in the system, and δ is the depth of the indentation of the tip. The point-to-point search method is used to find the contact point between the microcapsules and the tip through Matlab. The force-distance curve behind the contact point can be used to calculate the slope and finally the Young's modulus. Scanning electron microscope

(SEM) were acquired on a HITACHI UHR FE2SEM SU8000. The hydrogen spectra of polymers were measured by ^1H NMR. 5-10 mg of the sample was dissolved in the CDCl_3 (0.5 mL), and the sample was tested by Bruker's Avance-400 MHz NMR spectrometer. The test result was analyzed by MestRec. Gel Permeation Chromatography (GPC) was performed with a Hitachi L-2130 HPLC pump using molecular weight and polydispersity, the Hitachi L-2350 oven was operated at 40 °C. The GPC eluent was a flow HPLC grade DMF rate of 1.0 mL min⁻¹. X-ray photoelectron spectroscopy XPS was operated using a PHI ESCA 5700 with Al K α (1486.6 eV). The Samples for XPS and Raman measurements were prepared by drying different sample solutions on a silicon wafer. TGA/SDTA851e was purchased at METTLER TOLEDO. Optical microscope image is recorded on a Leica DMI8. Confocal image was obtained on a Leica SP8 laser confocal scanning microscope. UV-vis spectra were purchased on a PerkinElmer spectrophotometer (Lambda 750S, USA). Samples for UV-vis were using a microquartz cuvette over a wavelength range of 200–800 nm. Dynamic light scattering DLS were carried out at 25°C using a ZETASIZER Nano series instrument (Malvern Instruments, UK).

3. Experimental section

3.1 Synthesis of Au NPs

A 250 ml three-neck round bottom flask was boiled by adding 2.2 mM sodium citrate and 150 ml of water and vigorously stirred for 15 minutes. The increase in condenser was beneficial to inhibit evaporation of the solvent. After starting to boil, 1 mL of HAuCl_4 (25 mM) were injected. The color of the solution changed from yellow to a soft pink within 10 minutes. The container was immediately cooled until the solution temperature reached 90°C. Then, 1mL of sodium citrate (60 mM) and 1mL of HAuCl_4 solution (25 mM) were injected in sequence (once every two minutes). By repeating the process (adding 1 mL of 60 mM sodium citrate and 1 mL of 25 mM HAuCl_4 in sequence), up to 14 generations of progressively larger gold particles were grown. The centrifuged gold nanoparticles were further characterized by transmission electron microscopy (TEM) and UV-vis spectroscopy.

3.2 Synthesis of PNIPAAm by RAFT polymerization

The PNIPAAm were prepared according to the foregoing description³. RAFT agent (10 mg), NIPAAm (344.3 mg), AIBN (1.2 mg) were dissolved in acetonitrile and added to a 10 mL of round bottom flask. The round bottom flask was sealed with a rubber stopper wrapped with a sealing film to remove oxygen by nitrogen for 30 min. Polymerization was carried out in an oil bath at 65 °C for 8 hours. The product was further purified in diethyl ether/hexane. The PNIPAAm was characterized by ¹HNMR spectroscopy in CDCl₃. The proton signal (δ , 4H, 2.8-3.0 ppm) from succinimide in the PNIPAAm chain was clearly visible in the ¹HNMR spectrum. The molecular weight of the PNIPAAm was determined by ¹HNMR by comparing the proton signal $\delta = 2.9$ ppm in the integrated succinimide with the characteristic CH signal of $\delta = 4.0$ ppm in the repeating unit of NIPAAm (M_n , 10,000 g mol⁻¹).

3.3 Synthesis of gold nanoparticles microcapsules

1 mL of purified gold nanoparticles were pipetted into a 10 mL screw bottle, and PNIPAAm (20 mg) and mPEG2k-SH (10 mg) were weighed in sequence and ultrasonication was performed for 10 min to prevent any agglomeration. Stir the mixed solution for 10 hours to form the polymer conjugated gold nanoparticles (PEG-Au NPs-PNIPAAm). Then the mixed solution was purified by centrifugation multiple times to remove excess polymers. The gold nanoparticles microcapsules were prepared by mixing an aqueous PEG-Au NPs-PNIPAAm solution (20 μ L) with 2-ethyl-1-hexanol (100 μ L) followed by shaking the mixture for 40 S. Finally, a W/O gold nanoparticles microcapsules solution was obtained. In addition, it is interesting to mention that the Au NPs microcapsule could be also generated by mixing PEG-Au NPs-PNIPAAm with different oil phase at a water/oil volume fraction (ϕ_w) of 0.20 including chloroform, carbon tetrachloride, glyceryl tributyrate, triacetin, triolein, dodecane, while after 30 min incubation, only by using glyceryl tributyrate as the oil phase could give a stable microcapsule system.

The whole preparation procedure of the microcapsules is followed to the Pickering emulsion technique. It is well-known that Pickering emulsion utilizes solid particles alone as stabilizers, which accumulate at the interface between two immiscible liquids

and stabilize droplets against coalescence. The formation of a steric barrier by the solid particle-based building blocks adsorbing at the oil–water interface is the main driving force for the self-assembly. That is, building blocks are able to irreversibly attach to the oil–water interface, leading to a more efficient stabilization than surfactant adsorption⁴. The wettability of the building blocks at the oil–water interface plays a key role on type of the emulsions either oil-in-water or water-in-oil Pickering emulsion, as well as the stability of the formed microcapsules. This is also well supported by the control experiment that by increasing the content of PNIPAAm in the building blocks (mass ratios PEG:PNIPAAm in the building block from 5/1, 2/1, 1/1, 1/2 to 1/3) to increase the wettability to the oil phase, a more stabilized microcapsule can be obtained.

3.4 Enzyme activity test by using the substrate of 4-Nitrophenyl phosphate disodium salt hexahydrate (pNPP)

A reaction solution containing 25 mmol of triethanolamine, 1 mmol of magnesium chloride, pNPP (50 μL , 1 mg mL^{-1}) and ALP (50 μL , 1 mg mL^{-1}) was added to the EP tube. The reaction was allowed to stand at from 25 °C to 85 °C for half an hour, then 0.1 M, 100 μL of sodium hydroxide was added to terminate the reaction, and the OD value was measured by a microplate reader at a wavelength of 405 nm. The OD value of the sample was read on the ALP standard curve (U mL^{-1}).

ALP standard curve plotting: 11 mg of 4-nitrophenol in methanol (4-NP) was soaked and dissolved in distilled water to 25 ml, and the concentration of 4-NP was 3.20 $\mu\text{mol mL}^{-1}$. Dilute the enzyme to 1.60 $\mu\text{mol mL}^{-1}$, 0.80 $\mu\text{mol mL}^{-1}$, 0.40 $\mu\text{mol mL}^{-1}$, 0.20 $\mu\text{mol mL}^{-1}$, 0.10 $\mu\text{mol mL}^{-1}$ and 0.05 $\mu\text{mol mL}^{-1}$ equivalent to ALP 6.4 U mL^{-1} , 3.2 U mL^{-1} , 1.6 U mL^{-1} , 0.80 U mL^{-1} , 0.40 U mL^{-1} and 0.20 U mL^{-1} (activity value). The OD value of 4-NP was measured by a microplate reader at a wavelength of 405 nm. A linear regression equation was obtained by taking the ALP activity value as an independent variable and using the corresponding OD value as a dependent variable.

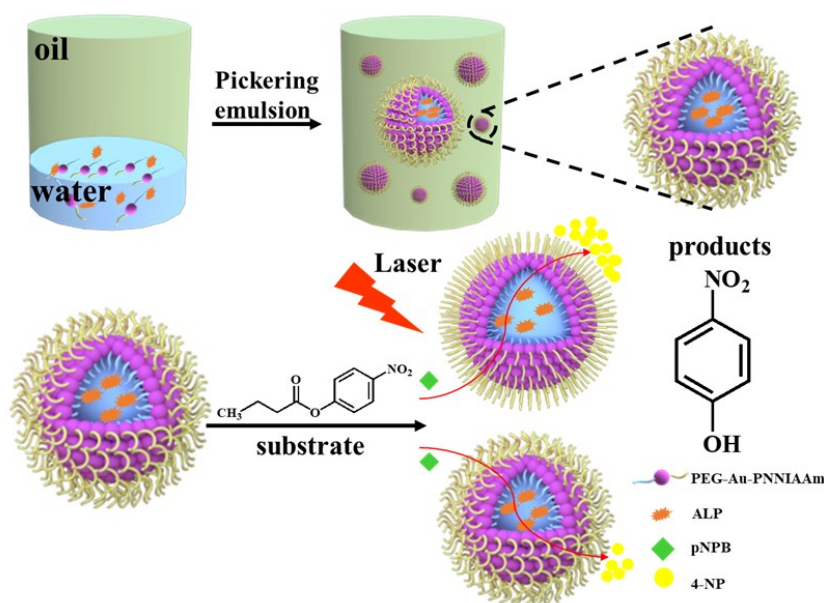
3.5 Labelling alkaline phosphatase by green fluorescence dye

10 mg of alkaline phosphatase was dissolved in 3 mL of pH 8.5 sodium carbonate

buffer. 50 μL of Fluorescent isothiocyanate (1 mg mL^{-1} , in DMSO) was added to the Erlenmeyer flask. The reaction was stirred overnight in the dark, then dialyzed against deionized water, and finally freeze dried.

3.6 Determination of the interfacial enzyme reaction in the Au NPs microcapsule

Alkaline phosphatase (ALP, 50 μL , 10 mg mL^{-1}) was encapsulated into the interior of the Au NPs microcapsule, and then the substrate 4-nitrophenylbutyric (pNPB, 10 μL , 10 mg mL^{-1}) and 200 μL of buffered solution (25 mmol of triethanolamine, 1 mmol of magnesium chloride) was added to the microcapsule (100 μL) solution for interfacial catalytic reaction.



Scheme S1 Schematic illustration of the synthesis of the Au NPs microcapsules based on Pickering emulsion strategy with enhanced interfacial catalytic reaction rate of the encapsulated alkaline phosphatase triggered by near-infrared irradiation.

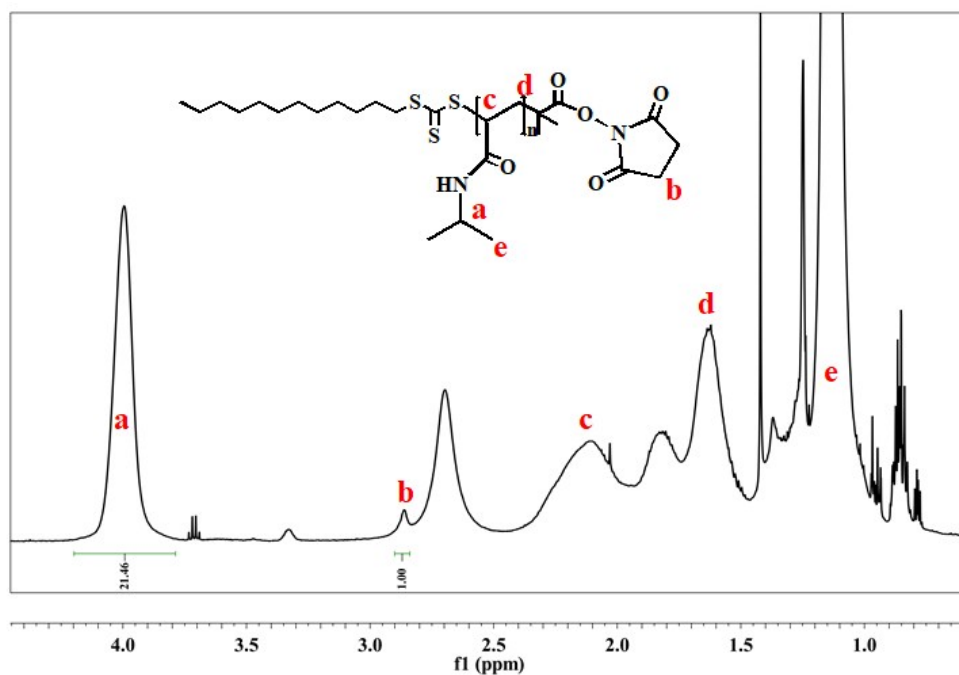


Figure S1. ¹H NMR spectrum of PNIPAAm (M_n 10000 g mol^{-1} , PDI 1.06) in CDCl_3

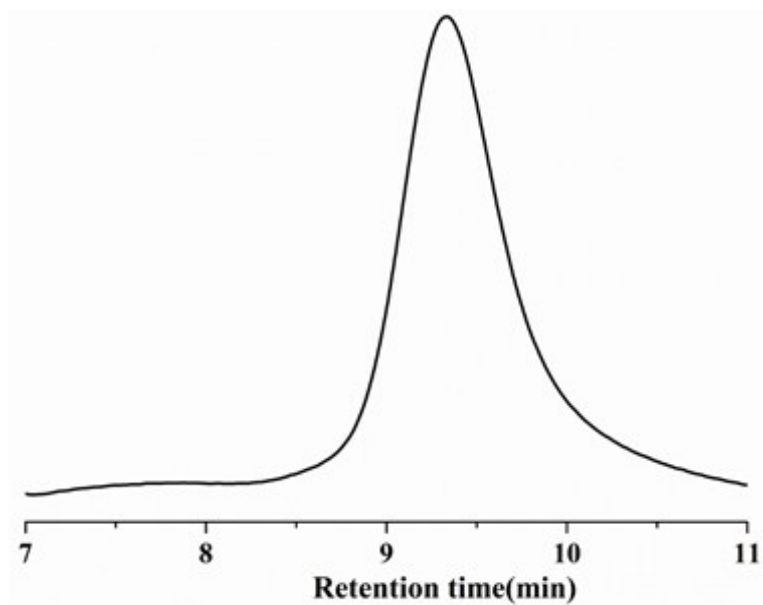


Figure S2. GPC profile of PNIPAAm. N, N-Dimethylformamide (DMF) was used as the eluent with the PNIPAAm concentration of 1.0 mg mL^{-1} . The PDI value was 1.06.

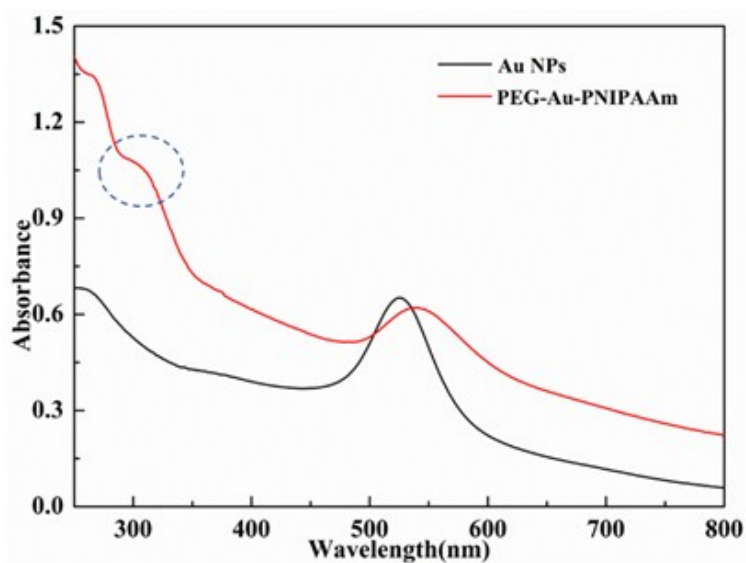


Figure S3. The UV-vis spectrum of Au NPs (black curve) and gold polymer conjugate (PEG-Au NPs-PNIPAAm, red curve), respectively. The characteristic peak of gold nanoparticles is around 550 nm, the characteristic absorption peaks of PNIPAAm are circled in blue at 308 nm.

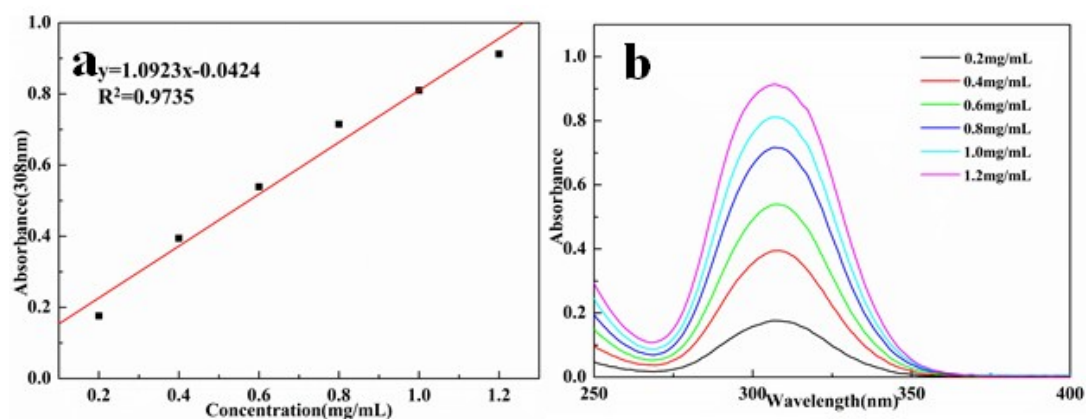


Figure S4. (a) Calibration curve of UV-vis absorbance for PNIPAAm at 308 nm; (b) Different concentrations of UV absorption of PNIPAAm. The ultraviolet spectrum of PNIPAAm at 0.2 mg mL^{-1} , 0.4 mg mL^{-1} , 0.6 mg mL^{-1} , 0.8 mg mL^{-1} , 1.0 mg mL^{-1} , 1.2 mg mL^{-1} was determined. According to Lambert's law, the calibration curve of PNIPAAm was obtained. By substituting the calibration curve, it can be concluded that the concentration of PNIPAAm in PEG-Au NPs-PNIPAAm was 0.95 mg mL^{-1} .

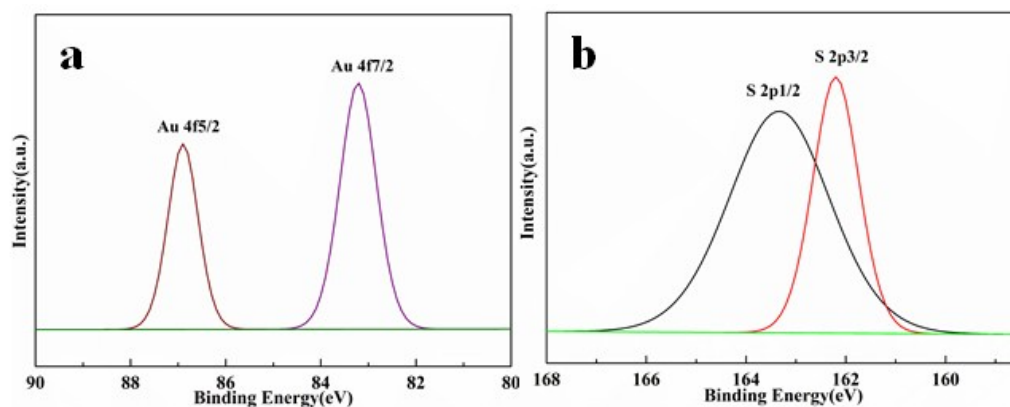


Figure S5. X-ray photoelectron spectroscopy (XPS) spectra of (a) Au 4f, and (b) S 2p. The gold nanoparticles conjugated by the polymers were combined on the surface of the ruthenium by the form of Au-S bond. When the photoelectron angle was 5 degrees, the Au 4f region spectrum was measured, where 84.0 eV and 87.7 eV correspond to Au 4f 7/2 and Au 4f 5/2, respectively. The S 2p region spectrum obtained at 5 degrees had a broad broadening of the XPS peak, indicating that the sulfur element in the sample may exist in two different chemical forms, indicating that the sulfur XPS spectrum in the sample was from two at 162.6 eV and 164.5 eV. The peaks were superimposed to confirm the formation of the Au-S bond.

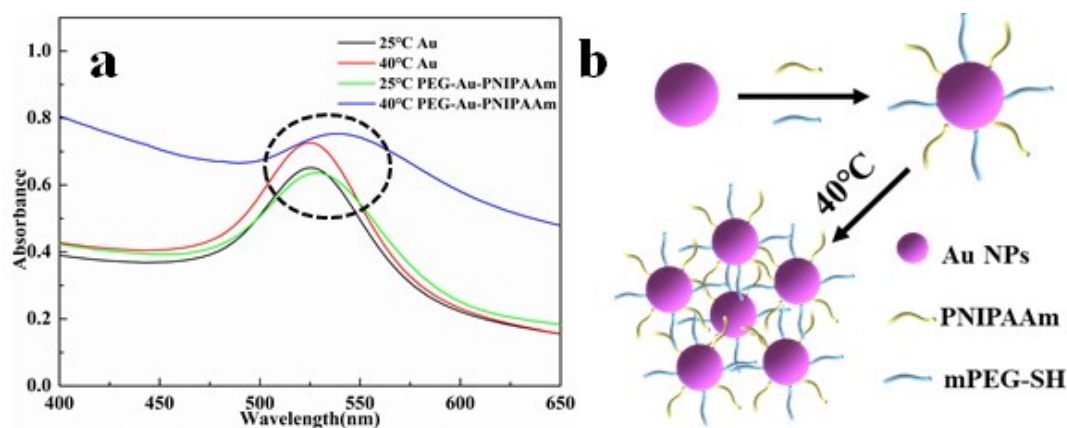


Figure S6. (a) UV-vis spectra of Au NPs, PEG-Au NPs-PNIPAAm at 25 °C or 40 °C, respectively. (b) Schematic illustration of PEG-Au NPs-PNIPAAm aggregation by changing the temperature from 25 °C to 40 °C. Au NPs and PEG-Au-PNIPAAm at 25 °C and 40 °C, UV-vis spectra measurement was employed, where the PEG-Au-

PNIPAAm peak of SPR had a obviously red shift compared to Au NPs when the temperature was raised from 25 °C to 40 °C. we attribute the absorbance increase and red shift in the peak of SPR to the shrinkage of the PNIPAAm chain which may cause its entanglement onto Au NPs due to the increase in temperature, thus eventually resulting in an increase in scattered light and aggregation of gold nanoparticles.

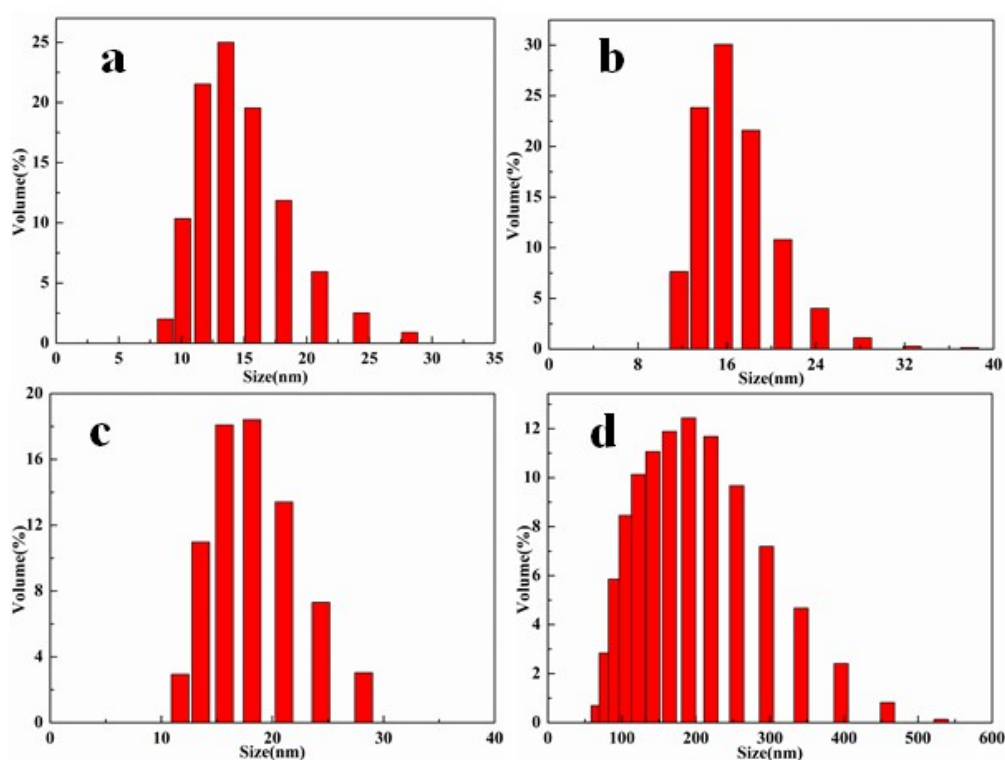


Figure S7. Particle size distribution of (a) 25 °C Au NPs. (b) 40 °C Au NPs. (c) 25 °C PEG-Au NPs-PNIPAAm. (d) 40 °C PEG-Au NPs-PNIPAAm. When the gold nanoparticles solution was raised from 25 °C to 40 °C, the size of the gold nanoparticles does not change, and when the PEG-Au NPs-PNIPAAm was raised to 40 °C, the size of the gold nanoparticle conjugates increased due to the temperature induced phase transition of the PNIPAAm.

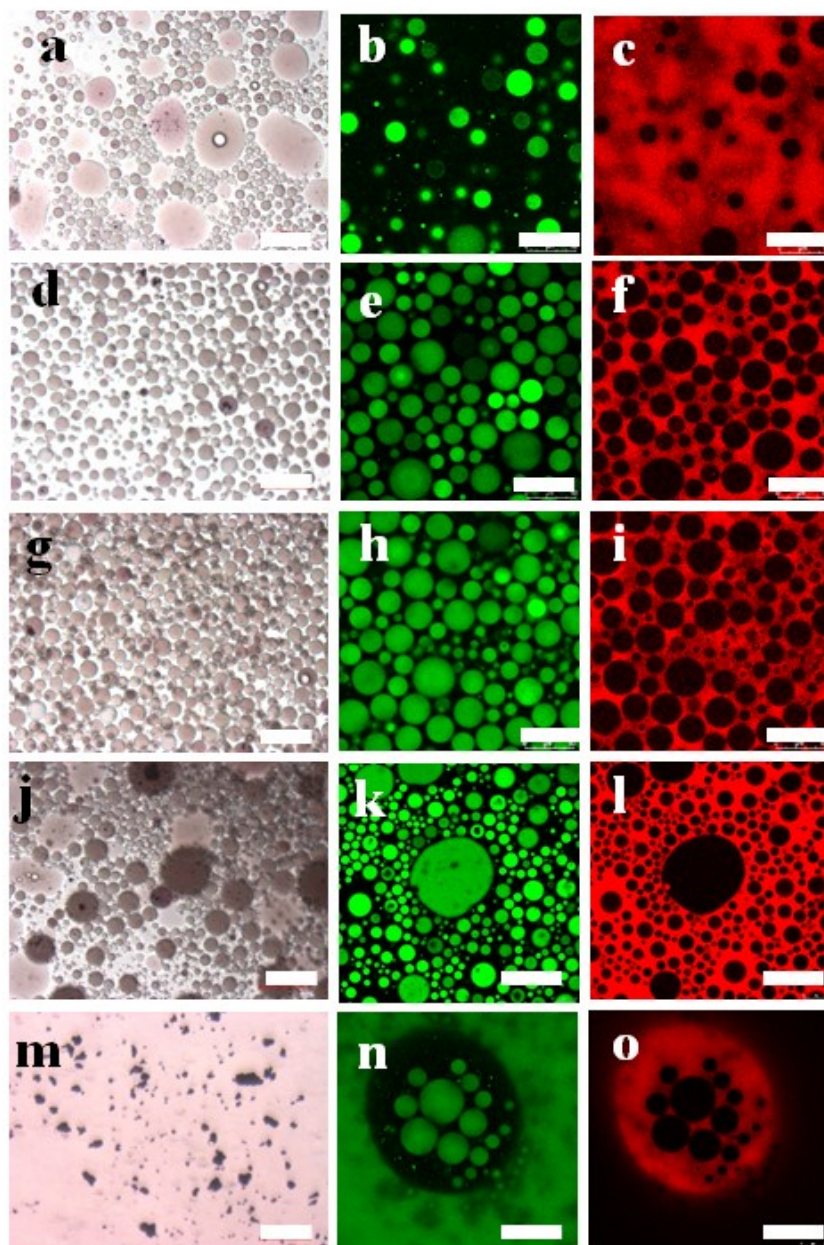


Figure S8. Optical and fluorescence microscope images of Au NPs microcapsules prepared by using different oil/water ratios of (a-c) 400 μL : 20 μL (20: 1). (d-f) 100 μL : 20 μL (5: 1). (g-i) 20 μL : 20 μL (1: 1). (j-l) 20 μL : 100 μL (1: 5). (m-o) 20 μL : 400 μL (1: 20). Scale bar is 100 μm for microscope images (left column), scale bar is 25 μm for confocal images (the right two columns). The aqueous phase was marked by fluorescein dye and the oil phase by Nile red. It can be concluded that the Au NPs-based microcapsules were stable at a water/oil volume fraction (ϕ_w) of 0.20.

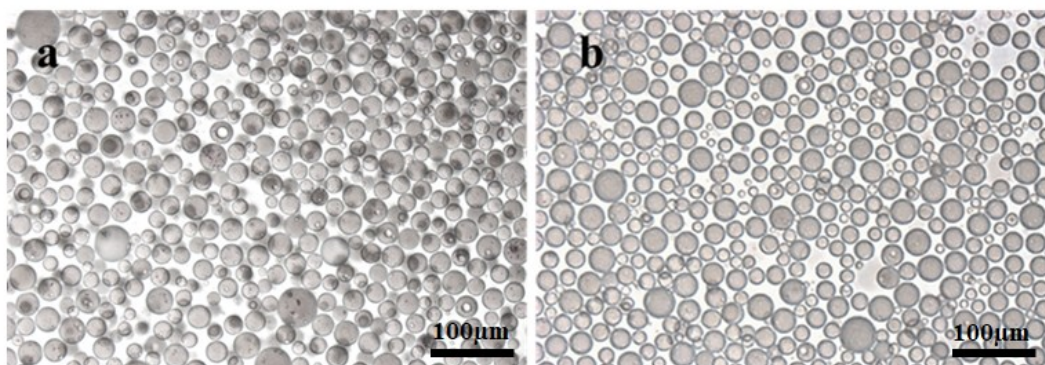


Figure S9. Microscope images of the Au NPs microcapsules were taken at different times (a) 30 min. (b) 4 weeks. The gold nanoparticle microcapsules were in the form of hollow spherical microstructures, which was structurally stable and remain spherical shape for four weeks at room temperature.

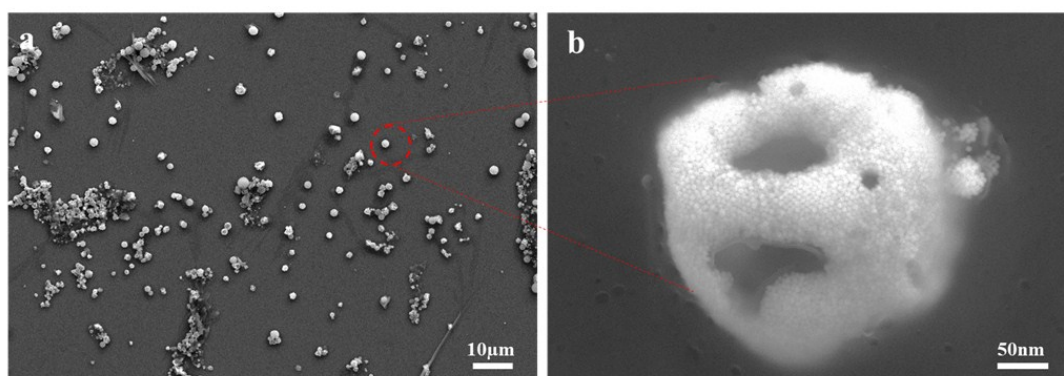


Figure S10. SEM images showing (a) intact Au NPs microcapsules, and (b) magnified image of the marked area in (a) showing microcapsules assembled from gold nanoparticles.

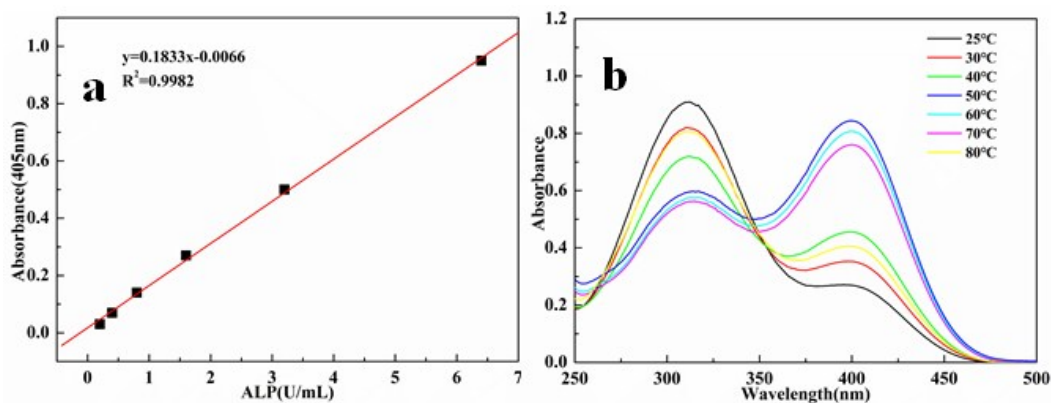


Figure S11. (a) Corresponding calibration curve based on plotting the absorbance at 405 nm against the concentration of alkaline phosphatase (ALP). (b) The UV-Vis spectrum of the obtained ALP activity from 25 °C to 80 °C. A reaction mixture of pNPP (50 μ L, 1 mg mL⁻¹) and ALP (50 μ L, 1 mg mL⁻¹) was added to the EP tube, and it was allowed to stand at 37 °C for half an hour in the dark. Then 100 μ L of 0.1 M sodium hydroxide was added, and the reaction was terminated by enzyme-labeled instrument to determine the OD value at 405 nm. The enzyme activity value was calculated by the calibration curve. The difference in ultraviolet absorption values corresponding to changes in enzyme activity of the ALP enzyme at 25 °C to 80 °C was measured. As the temperature rose to 50 °C, the enzyme activity reached a maximum of 4.56 U mL⁻¹. However, when the temperature was further increased to 80 °C, the enzyme activity began to decrease to 2.22 U mL⁻¹.

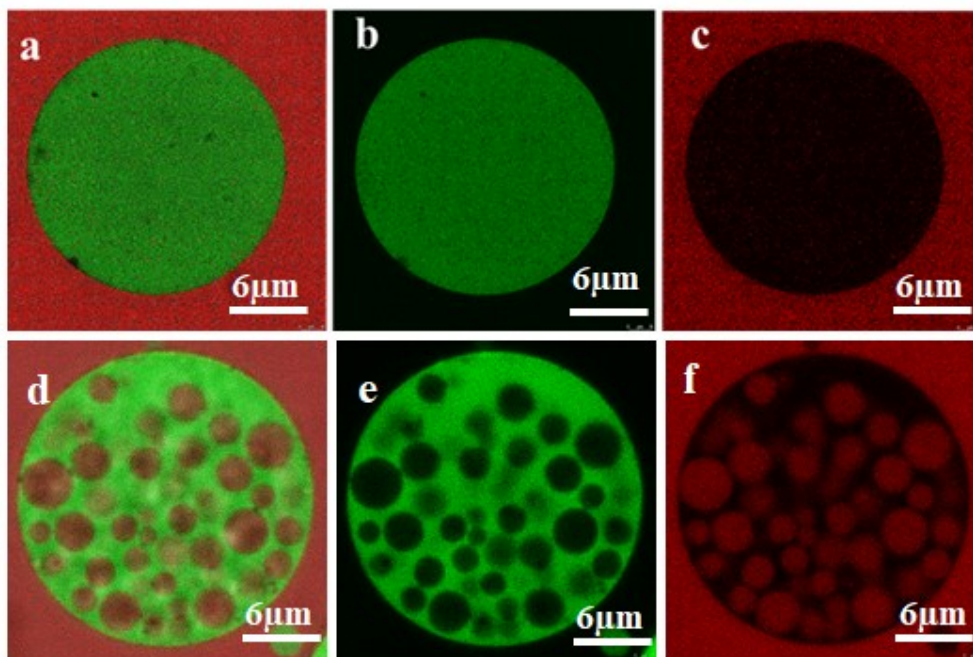


Figure S12. Fluorescence confocal microscopy images of ALP encapsulated inside the Au NPs microcapsules with adding pNPB as substrates. ALP was labeled by green fluorescent (FITC) dye and the oil phase by Nile red. (a-c) without pNPB and NIR. (d-f) by adding pNPB in the NIR. Confocal microscopy images showed green fluorescence inside the microcapsule, indicating that alkaline phosphatase was encapsulated within the microcapsule, and Nile red labeled oil phase is external. Taking the heat sensitive characteristics of PNIPAAm into account, the photothermal effect of gold nanoparticles made PNIPAAm more hydrophobic and thus increased interfacial catalytic efficiency.

References

1. H. Xie, D. S. Haliyo and S. Régnier, *Nanotechnology*, 2009, **20**, 215301.
2. Sader J E, Chon J W M, Mulvaney P. *Review of Scientific Instruments*, 1999, **70** (10): 3967-3969.
3. X. Huang, M. Li, D. C. Green, D. S. Williams, A. J. Patil and S. Mann, *Nat. Commun.*, 2013, **4**, 2239.
4. Monegier du Sorbier et al., *J. Colloid Interface Sci.* 2015, **448**, 306–314.